

Electrogenerated chemiluminescence peptide-based biosensing method for cardiac troponin I using peptide-integrating Ru(bpy)₃²⁺-functionalized gold nanoparticles as nanoprobe

Manman Dong¹ · Min Li¹ · Honglan Qi¹ · Zhejian Li¹ · Qiang Gao¹ · Chengxiao Zhang¹

Published online: 26 March 2015

© The Author(s) 2015. This article is published with open access at SpringerLink.com

Abstract A sensitive electrogenerated chemiluminescence peptide-based (ECL-PB) biosensing method for the determination of protein was developed by employing peptide-integrating Ru(bpy)₃²⁺ (bpy=2,2'-bipyridine)-functionalized gold nanoparticles (Ru(bpy)₃²⁺-AuNPs-peptide) as nanoprobe. Cardiac troponin I (cTnI), a reliable clinical biomarker for the detection of cardiac injury, was chosen as target protein, while a specific binding peptide (CFYSHSFHENWPS) was used as molecular recognition element. AuNPs were firstly functionalized with Ru(bpy)₃²⁺ through electrostatic interactions between citrate-capped AuNPs and Ru(bpy)₃²⁺ to form Ru(bpy)₃²⁺-AuNPs aggregates and then functionalized with peptide through Au-S bounds to form Ru(bpy)₃²⁺-AuNPs-peptide nanoprobe. AuNPs not only can capture numerous signal-generating molecules, resulting in high ECL intensity but also can capture a significant amount of the peptide, providing poly binding motif. The specific capture peptide was self-assembled on the surface of a gold electrode and then incubated with the target cTnI and Ru(bpy)₃²⁺-AuNPs-peptide successively. A sandwich-type peptide/cTnI/Ru(bpy)₃²⁺-AuNPs-peptide conjugate was formed on the surface of the electrode and an ECL signal was obtained in the presence of tri-*n*-propylamine. The novel biosensing method facilitates the sensitive detection of cTnI in the range from 3.0×10^{-12} g mL⁻¹ to $7.0 \times$

10^{-11} g mL⁻¹ with a low detection limit of 0.5 pg mL⁻¹. This work provides a promising strategy for the determination of proteins with simplicity, high sensitivity, and selectivity.

Keywords Electrogenerated chemiluminescence · Biosensing · Peptide · Cardiac troponin I · Gold nanoparticles

Introduction

Cardiac troponin I (cTnI), a part of the troponin complex present in cardiac muscle tissues, is a reliable biomarker of cardiac muscle tissue injury and is widely used in the early diagnosis of acute myocardial infarctions [1, 2]. Although an increase in cTnI concentration from 10 pg mL⁻¹ to over 1 ng mL⁻¹ into blood vessels within a few hours occurs during the damage to cardiac muscles, it is present at ultralow levels following the onset of acute myocardial infarction symptoms. Therefore, it is needed to develop sensitive methods for monitoring cTnI concentration during early stages [3]. Up to now, a lot of methods have been utilized in the determination of cTnI such as colorimetric [4, 5], fluorescent [6, 7], electrochemical [8, 9], chemiluminescence [10], and electrogenerated chemiluminescence (ECL) [11–14]. Among them, ECL has attracted attention in protein biosensing due to advantages such as a very low background signal, high sensitivity, and good temporal and spatial control [15, 16]. For example, two ECL immunosensors were reported by Cui et al. for human cTnI detection using luminol and *N*-(aminobutyl)-*N*-(ethylisoluminol)-functionalized gold nanoparticles (AuNPs) as signals [11, 12]. An ECL immunoassay was developed by Smith for the detection of rat TnI in serum [13]. Ruan reported an ECL immunosensor for the detection of cTnI by using self-enhanced ECL luminophore [14]. ECL immunoassays are typically conducted by employing

Electronic supplementary material The online version of this article (doi:10.1007/s13404-015-0156-2) contains supplementary material, which is available to authorized users.

✉ Honglan Qi
honglanqi@snnu.edu.cn

¹ Key Laboratory of Analytical Chemistry for Life Science of Shaanxi Province, School of Chemistry and Chemical Engineering, Shaanxi Normal University, Xi'an 710062, People's Republic of China

antibodies as molecular recognition elements. However, antibodies exhibit certain limitations. For instance, the expensive production in mammalian cells and the stability in harsh environments of the antibody make it desirable to seek alternative affinity molecules [17].

Short linear binding peptides selected using phage display techniques have received much attention in protein analysis due to the cost-effective synthesis, stability and resistance to harsh environments, and facile molecular level amenability, as compared to antibodies [18]. A linear peptide (with the sequence FYSHSFHENWPS) was first selected using polyvalent phage display by Park et al. that could selectively bind to human cTnI with nanomolar affinity [19]. A homogeneous ECL peptide-based method for the detection of cTnI has been developed in our lab using the specific peptide as a molecular recognition element [20]. However, the sensitivity is limited because one ECL signal per peptide is employed. We recently reported a homogeneous ECL method for cTnI using liposomes as carriers of the ECL signal reagent, in which a low detection limit of 4.5 pg mL^{-1} was obtained for cTnI because liposomes can encapsulate large amounts of reporter molecules (1.9×10^7 ruthenium derivatives/liposome) [21]. Compared with conventional ECL methods with one label per recognition element, the aforementioned technologies show enormous signal amplification, but the complicated labeling and analytical procedures required the need for novel, simple, and sensitive methods for cTnI in clinical settings.

Since the use of AuNPs for biological uses was first demonstrated by Mirkin et al. in 1996 [22], AuNPs have been widely used in the design of biosensors [23–25]. Generally, AuNPs are employed in the modification of electrodes [26, 27] as they provide a large surface area and facilitate the electron transfer between active molecules and electrodes. Moreover, AuNPs have been employed as carriers for conventional signals such as luminol [11, 28] and ruthenium complexes [29] thus affording ECL signal amplification. Since many luminol moieties with chemiluminescence activity were coated on the surface of the AuNPs, a low detection limit of 2 pg mL^{-1} for cTnI was obtained via the signal amplification by the AuNPs. Tris(2,2'-bipyridine) dichlororuthenium(II) ($\text{Ru}(\text{bpy})_3^{2+}$) has received considerable attention as an ECL signal reagent because of its higher luminescence yield and good electrochemical and photochemical stability [30]. AuNPs can be functionalized with $\text{Ru}(\text{bpy})_3^{2+}$ and derivatives via electrostatic interactions or self-assembly and have been used in chemical sensors [31–33], immunosensors [34], DNA biosensors [35–37], and cell bioassay [38].

With our interest in the development of ECL peptide-based (ECL-PB) biosensors, we design a peptide-integrating $\text{Ru}(\text{bpy})_3^{2+}$ -functionalized gold nanoparticles ($\text{Ru}(\text{bpy})_3^{2+}$ -AuNPs-peptide) nanoprobe and develop a sensitive and

simple method for the detection of cTnI (Fig. 1). In this work, the characteristics of $\text{Ru}(\text{bpy})_3^{2+}$ -AuNPs and $\text{Ru}(\text{bpy})_3^{2+}$ -AuNPs-peptide and the analytical performance toward cTnI are presented.

Experimental

Reagents and apparatus

Peptide CFYSHSFHENWPS (MW=1640.77, Fig. S1 in Supporting Information) was designed according to Park et al. [19], which contained a terminal thiol-containing cysteine residue to facilitate self-assembly on the surface of the gold electrode or AuNPs, and purchased from Sinoasis Pharmaceuticals, Inc. (China). Cardiac troponin I (cTnI, human heart) and skeletal troponin I (sTnI) were obtained from Abcam Inc. (Cambridge, UK). C-Reactive protein (CRP), chloroauric acid (HAuCl_4), tris(2,2'-ripyridine) dichlororuthenium(II) ($\text{Ru}(\text{bpy})_3\text{Cl}_2$, $\text{Ru}(\text{bpy})_3^{2+}$), and bis(2,2'-bipyridine)-4,4'-dicarboxybipyridine-ruthenium di(*N*-succinimidyl ester) bis(hexafluorophosphate) (RuI) were obtained from Sigma-Aldrich (USA). Albumin chicken egg protein was obtained from Sino-American Biotechnology Co., Ltd. (China). Prostate-specific antigen (PSA) was purchased from Fitzgerald Industries International, Inc. (USA). Human immunoglobulin G (IgG) and bovine serum albumin (BSA) were obtained from Beijing Biosynthesis Biotechnology Co., Ltd. (China). 6-Mercapto-1-hexanol (MCH), tripropylamine (TPA), and sodium citrate were purchased from Sinopharm Chemical Reagent Co., Ltd (China).

Phosphate-buffered saline (PBS; 0.1 M) consisted of 0.1 M NaH_2PO_4 , 0.1 M Na_2HPO_4 , and 0.1 M KCl (pH 7.4). Phosphate buffer (PB; pH 7.4; 10 mM) contained 10 mM NaH_2PO_4 , and 10 mM Na_2HPO_4 was used as the washing buffer. Other reagents were of analytical grade, and millipore Milli-Q water (18.2 M Ω cm) was used in this work.

ECL and electrochemical setups were similar to those in our previous work [27]. The integrated ECL imaging system included a CHI 660 electrochemical workstation (Shanghai Chenhua Instrument Co. Ltd., China) suitable for the needed potential for the ECL-triggered reaction, an Olympus IX-51 inverted microscope (Olympus corporation, Tokyo, Japan) and a Magnafire model iXon + DU-897 Andor EMCCD (Andor Technology Ltd., Belfast, Northern Ireland). A JEM-2100 transmission electron microscope (JEOL, Japan) was used to obtain transmission electron micrograph (TEM) images. Atomic force micrograph (AFM) images were obtained with a CSPM5500 Scanning Probe Microscope (Being Nano-Instruments, Ltd. China).

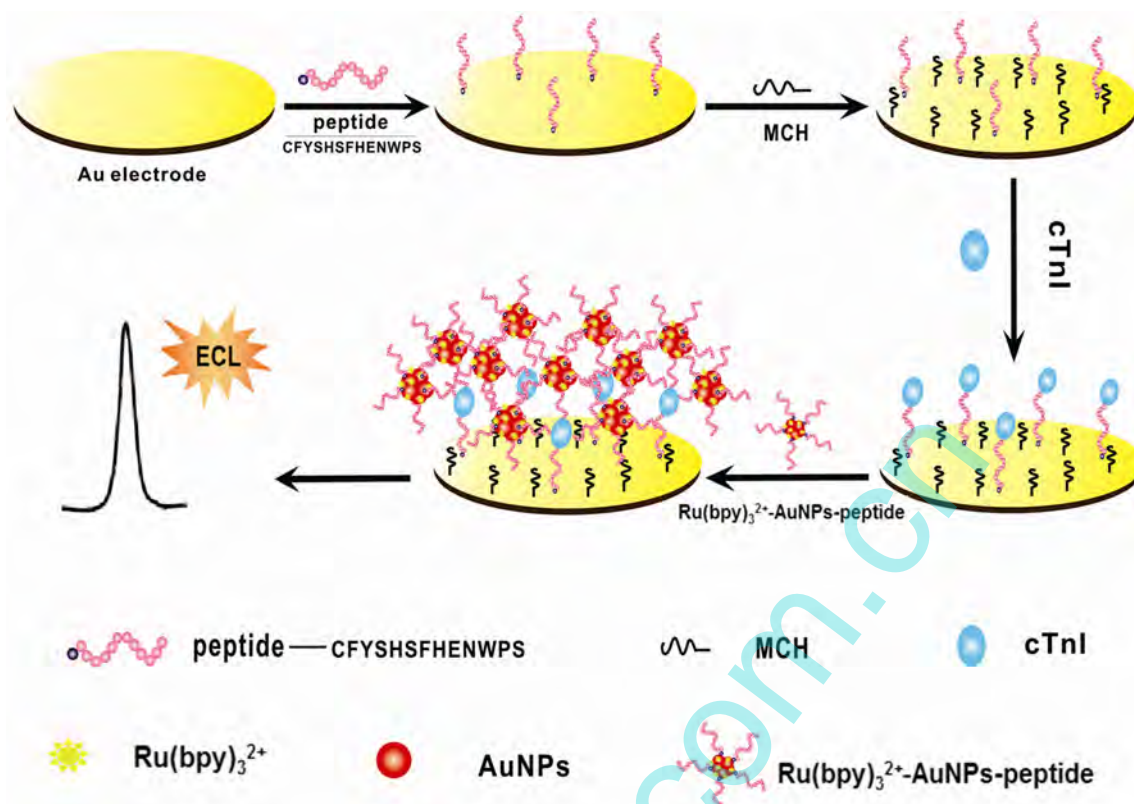


Fig. 1 Scheme of the fabrication of the ECL peptide-based biosensor and ECL detection of cTnI

Preparation of Ru(bpy)₃²⁺-AuNPs and Ru(bpy)₃²⁺-AuNPs-peptide

AuNPs with a diameter of ~12 nm were prepared by citrate reduction of HAuCl₄ in an aqueous solution according to Frens's work [39]. In brief, 100 mL of 0.01 % HAuCl₄ was heated to boiling, and then, 4 mL of 1 % (3.4 × 10⁻² M) sodium citrate was added under stirring. The solution was boiled for another 30 min and subsequently left to cool to room temperature. The obtained AuNPs were stored in a dark glass bottle at 4 °C until use.

AuNPs were firstly functionalized with Ru(bpy)₃²⁺ through electrostatic interactions between citrate-capped AuNPs and Ru(bpy)₃²⁺ to form Ru(bpy)₃²⁺-AuNPs aggregates and then functionalized with peptide through Au-S bonds to form peptide-integrating Ru(bpy)₃²⁺-functionalized gold nanoparticles (Ru(bpy)₃²⁺-AuNPs-peptide) nanoprobe. According to the process in the Sun's work [23], 100 μL of an aqueous solution of 10 μM Ru(bpy)₃Cl₂ was slowly added into 1.0 mL of AuNP solution under vigorous stirring at room temperature. The resulting precipitates were collected by centrifugation and re-suspended in 1.0 mL water with sonication to form Ru(bpy)₃²⁺-AuNPs aggregates (Ru(bpy)₃²⁺-AuNPs).

One milliliter of Ru(bpy)₃²⁺-AuNPs aggregates were mixed with 1.0 mL of 10 mM PB (pH 7.4) containing 1.2 × 10⁻⁴ M peptide and stirred gently overnight. The resulting

mixture was centrifuged and re-suspended in 1 mL of 10 mM PB (pH 7.4) to form peptide-labeled Ru(bpy)₃²⁺-AuNPs (Ru(bpy)₃²⁺-AuNPs-peptide). The resulting Ru(bpy)₃²⁺-AuNPs-peptide was stored at 4 °C until use.

The preparation of Ru(bpy)₂(dcbpy-NHS)(PF₆)₂-labeled peptide (Ru1-peptide) was carried out according to a procedure described previously [20].

Immobilization of capture probe

A gold electrode (2.0-mm diameter) was treated according to Carvalho et al. [40]. A cleaned gold electrode was immersed into 0.5 mL of 11.3 μM capture peptide solution for 2 h at room temperature and then thoroughly washed with 10 mM PB (pH 7.4). After that, the resulting electrode was immersed in 100 μL of 1 mM MCH for 30 min to block the uncovered surface of the electrode and was washed with 10 mM PB (pH 7.4) to obtain the peptide-modified electrode.

ECL measurements

First, the peptide-modified electrode was immersed into 100 μL of different concentrations of target cTnI and incubated for 60 min. Next, the resulting electrode was immersed into 100 μL 5-fold diluted Ru(bpy)₃²⁺-AuNPs-peptide solution and incubated for another 60 min. After each incubation step,

the electrode was rinsed thoroughly with 10 mM PB (pH 7.4) to remove adsorption components. The ECL measurement was performed at a constant potential of +0.95 V in 1.0 mL of 0.10 M PBS (pH 7.4) containing 50 mM TPA, and the initial cycle data was recorded. The concentration of cTnI was quantified by the increased ECL intensity ($\Delta I = I_s - I_0$), where I_0 is the ECL peak height in the absence of cTnI and I_s is the ECL peak height in the presence of cTnI. All experiments were carried out at room temperature.

ECL images were obtained in 1.0 mL of 0.10 M PBS (pH 7.4) containing 50 mM TPA under darkroom conditions. The surface of the working electrode faced the EMCCD detector, so that the light generated by the ECL reaction could reach the detector. A linear sweep voltammetry technique with a scan rate of 100 mV s^{-1} in the range of 0.6–1.1 V was applied to the working electrode, resulting in ECL. EMCCD control and image analysis were carried out using Andor SOLIS (v. 4.18, Andor Technology Ltd., Belfast, Northern Ireland).

Results and discussion

Characterization of $\text{Ru}(\text{bpy})_3^{2+}$ -AuNPs-peptide

In this work, $\text{Ru}(\text{bpy})_3^{2+}$ -AuNPs were firstly synthesized through electrostatic interactions between citrate-capped AuNPs and $\text{Ru}(\text{bpy})_3^{2+}$ in aqueous medium (as shown in Fig. 2a), and the formed $\text{Ru}(\text{bpy})_3^{2+}$ -AuNPs were characterized by UV–vis spectrum, fluorescence imaging, and TEM. The color of the AuNP solution is wine red (Fig. 2b, insert), and UV–vis spectrum of AuNPs gives a broad absorption at 523 nm (Fig. 2e) [41]. TEM shows that a well-dispersed AuNPs have an average diameter size of $\sim 12 \text{ nm}$ (Fig. 2b).

After treatment with $\text{Ru}(\text{bpy})_3^{2+}$, the color of $\text{Ru}(\text{bpy})_3^{2+}$ -AuNPs changed to purple (inset of Fig. 2c), and the absorption peak of $\text{Ru}(\text{bpy})_3^{2+}$ -AuNPs (537 nm) was red shifted by $\sim 16 \text{ nm}$ (Fig. 2f) [42]. This indicates that the aggregation of AuNPs occurs, attributed to the fact that the positively charged $\text{Ru}(\text{bpy})_3^{2+}$ serves as a cross-linking agent for negatively charged citrate-capped AuNPs [23]. The aggregation or

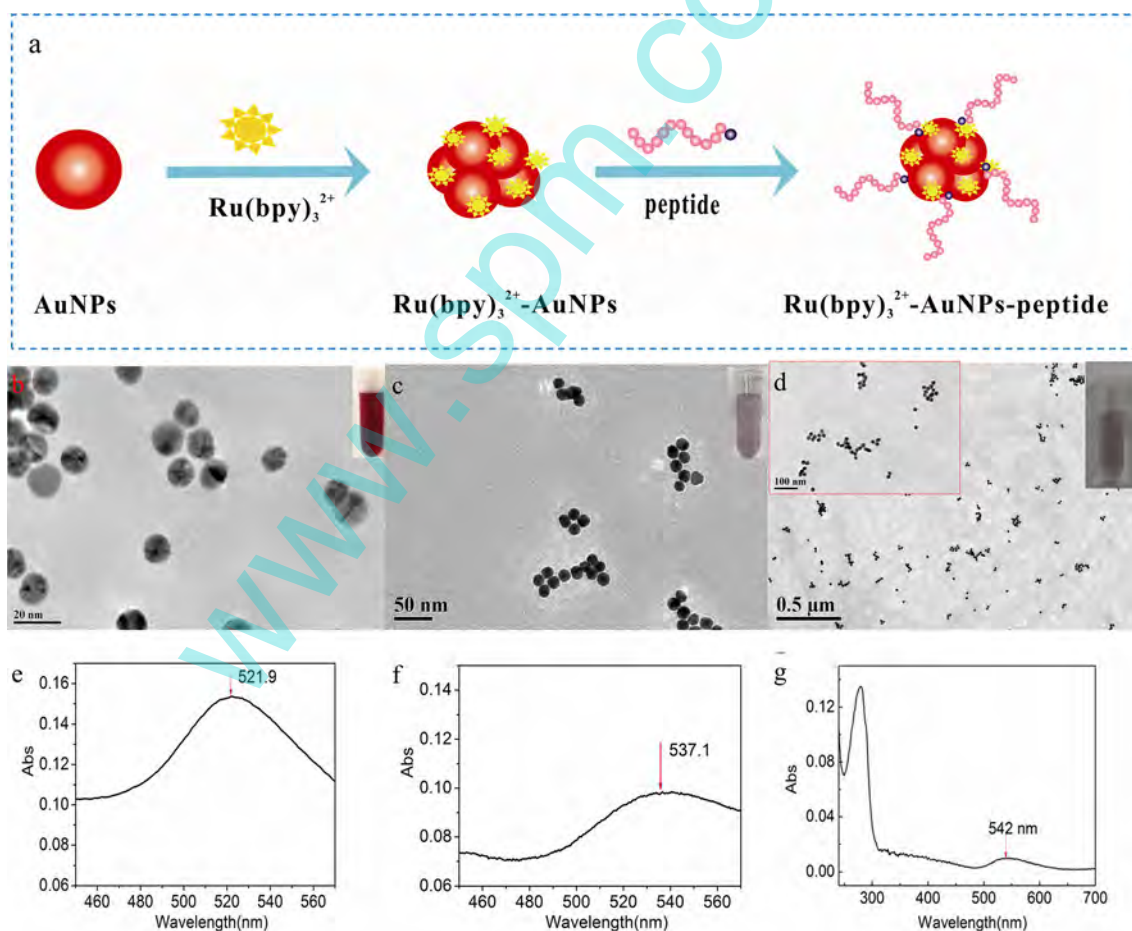


Fig. 2 a Scheme of the preparation of $\text{Ru}(\text{bpy})_3^{2+}$ -AuNPs-peptide. TEM images of citrate-capped AuNPs (b), $\text{Ru}(\text{bpy})_3^{2+}$ -AuNPs (c), and $\text{Ru}(\text{bpy})_3^{2+}$ -AuNPs-peptide (d). UV–vis spectra of citrate-capped AuNPs

(e), and $\text{Ru}(\text{bpy})_3^{2+}$ -AuNPs (f) and $\text{Ru}(\text{bpy})_3^{2+}$ -AuNPs-peptide (g). b Picture of citrate-capped AuNP solution, c picture of $\text{Ru}(\text{bpy})_3^{2+}$ -AuNPs solution, and d picture of $\text{Ru}(\text{bpy})_3^{2+}$ -AuNPs-peptide solution (insert)

flocculation of AuNPs upon addition of a “cross-linking” agent is well-documented [43]. The effective loading of $\text{Ru}(\text{bpy})_3^{2+}$ on the AuNPs could also be visualized via fluorescent imaging (see Fig. S2 in Supporting Information). The effect of concentration of $\text{Ru}(\text{bpy})_3^{2+}$ on the color of AuNPs was examined, and it was found that the color of AuNPs was changed from red to purple, and red to black precipitation change with the increase of $\text{Ru}(\text{bpy})_3^{2+}$ concentration from 10^{-5} to 0.05 M, respectively, which can be monitored by TEM and naked eyes (seen in Supporting Information Fig. S3). Here, 10^{-5} M $\text{Ru}(\text{bpy})_3^{2+}$ was employed when preparation of $\text{Ru}(\text{bpy})_3^{2+}$ -AuNPs in order to get stable and uniform ECL probe.

AuNPs not only provide an immobilized platform for $\text{Ru}(\text{bpy})_3^{2+}$ but also provide an immobilized platform for the peptide. The capture peptide was self-assembled on $\text{Ru}(\text{bpy})_3^{2+}$ -AuNPs via Au-S bonds yielding peptide- $\text{Ru}(\text{bpy})_3^{2+}$ -AuNPs nanoprobe and characterized by TEM, UV-vis spectrum, and visual picture. A slight aggregation occurs after the peptide conjugation, which was confirmed by the morphologies of $\text{Ru}(\text{bpy})_3^{2+}$ -AuNPs-peptide, as determined by TEM (Fig. 2d) and visual picture after the conjugation step (Fig. 2d, insert). UV-Vis spectra of the $\text{Ru}(\text{bpy})_3^{2+}$ -AuNPs-peptide showed the characteristic peaks at 280 and 542 nm, indicating that peptide has been self-assembled onto AuNPs (Fig. 2g).

Feasibility of the ECL-PB biosensing method for cTnI

Figure 1 shows the scheme of the fabrication of the ECL peptide-based biosensor and ECL detection of cTnI. A specific capture peptide was self-assembled on the surface of a gold electrode and then incubated with the target cTnI and $\text{Ru}(\text{bpy})_3^{2+}$ -AuNPs-peptide successively. A sandwich-type peptide/cTnI/ $\text{Ru}(\text{bpy})_3^{2+}$ -AuNPs-peptide conjugate was formed on the surface of the electrode. Cyclic voltammetry (CV) is a powerful tool to probe the nature of the modified electrodes by using $\text{Fe}(\text{CN})_6^{3-}/\text{Fe}(\text{CN})_6^{4-}$ couple as redox probe [44, 45]. A well-defined redox peak of $[\text{Fe}(\text{CN})_6]^{3-/4-}$ was obtained at bare gold electrode with a peak potential separation, ΔE , of 90 mV (see Fig. S4a). After the peptide and MCH were immobilized on the gold electrode, the oxidation peak current decreased to 27.2 μA , and the ΔE increased to 150 mV (see Fig. S4b). After the peptide-modified electrode was incubated with cTnI and $\text{Ru}(\text{bpy})_3^{2+}$ -AuNPs-peptide, the oxidation peak current further decreased to 25.5 and 15.0 μA , and the ΔE further increased to 170 mV (Fig. S4c) and 270 mV (Fig. S4d), respectively. The results indicate that the capture peptide can self-assemble on the bare gold electrode and the peptide-modified electrode can react with cTnI and $\text{Ru}(\text{bpy})_3^{2+}$ -AuNPs-peptide.

Figure 3 shows the ECL intensity-potential profiles with simultaneous CVs at different electrodes. In Fig. 3a, it can be

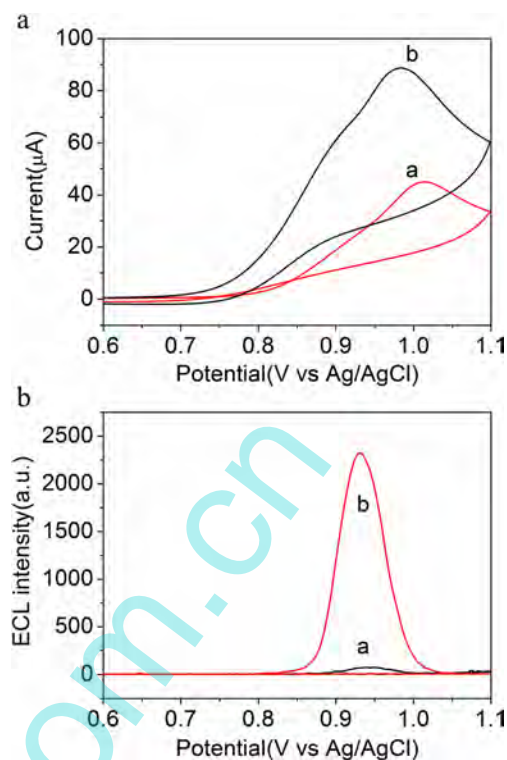


Fig. 3 Cyclic voltammograms (a) and ECL intensity-potential profiles (b) obtained at the peptide-modified gold electrode in 0.10 M PBS (pH 7.4) containing 50 mM TPA. **a** Peptide-modified gold electrode after incubation with 3.0×10^{-12} g mL $^{-1}$ cTnI. **b** Peptide-modified gold electrode after incubation with 3.0×10^{-12} g mL $^{-1}$ cTnI and $\text{Ru}(\text{bpy})_3^{2+}$ -AuNPs-peptide. Scan rate at 50 mV s $^{-1}$

seen that an irreversible oxidation peak appears at 1.01 V at the peptide-modified electrode incubating with cTnI, ascribed to the irreversible oxidation peak of TPA. An irreversible oxidation peak appears at 0.98 V after the peptide-modified electrode incubating with cTnI and $\text{Ru}(\text{bpy})_3^{2+}$ -AuNPs-peptide (Fig. 3b), respectively. A negative shift of the peak potential was observed at the peptide-modified electrode after incubation with cTnI and $\text{Ru}(\text{bpy})_3^{2+}$ -AuNPs-peptide, which may be ascribed to the presence of AuNPs on the electrode surface [46]. The increase of the oxidation peak current is ascribed to the reduction of $\text{Ru}(\text{bpy})_3^{2+}$ by TPA free radical formed during TPA oxidation [47]. A very low ECL signal (a.u. 73) was obtained at the peptide-modified electrode after incubation with cTnI (Fig. 3b, line a), while a relatively high ECL signal (a.u. 2336, 0.95 V) was obtained at the peptide-modified electrode after incubation with 3.0×10^{-12} g mL $^{-1}$ cTnI and $\text{Ru}(\text{bpy})_3^{2+}$ -AuNPs-peptide (Fig. 3b, line b). The original of this ECL peak at 0.95 V is ascribed to that TPA^+ (formed during TPA oxidation) oxidize $\text{Ru}(\text{bpy})_3^{2+}$ (formed from the reduction of $\text{Ru}(\text{bpy})_3^{2+}$ by TPA free radical) to give $\text{Ru}(\text{bpy})_3^{2+*}$ [47]. As such, $\text{Ru}(\text{bpy})_3^{2+}$ -AuNPs-peptide can be used as an ECL probe to determine cTnI.

In order to illustrate the amplification ability of AuNPs, Ru(bpy)₃²⁺-AuNPs-peptide and Ru1-peptide were employed as ECL probes (as shown in Fig. 4a), and the comparison of ECL responses of Ru1-peptide probe with that of Ru(bpy)₃²⁺-AuNPs-peptide probe was performed for target cTnI. Figure 4b shows the ECL intensity-potential profiles at different electrodes in 0.1 M PBS (pH 7.4) containing 50 mM TPA. A high ECL signal (7256 a.u.) is observed for 7.0×10^{-11} g mL⁻¹ cTnI using Ru(bpy)₃²⁺-AuNPs-peptide (line a). In contrast, a small ECL signal (3981 a.u.) is observed for a 10-fold higher level of cTnI (7.0×10^{-10} g mL⁻¹) using Ru1-peptide. The ECL intensity using Ru(bpy)₃²⁺-AuNPs-peptide as ECL probe is much larger than that of Ru1-peptide.

ECL imaging shows that both of the peptide-modified electrode using Ru(bpy)₃²⁺-AuNPs-peptide and Ru1-peptide as ECL probe can yield a detectable ECL signal (Fig. 4c, d). As such, the proposed ECL

method was viable for the determination of cTnI. The nonuniform ECL signal on the electrode surface may be ascribed to the heterogeneity of the electrochemical activity on the electrode surface [48] and the nonuniform distribution of Ru(bpy)₃²⁺ on the surface of the modified electrode. ECL counts also show that the ECL signal using Ru(bpy)₃²⁺-AuNPs-peptide as ECL probe is much higher than that of Ru1-peptide. This is attributed to the fact that Ru(bpy)₃²⁺-AuNPs-peptide not only captured numerous signal-generating molecules (Ru(bpy)₃²⁺ molecules), resulting in a high ECL signal, but also captured a significant amount of peptides, providing a sensing platform for cTnI [49, 50]. Moreover, AuNPs assembled on the electrode can also catalyze the ECL of the ruthenium complex/TPA system [51]. The signal amplification with Ru(bpy)₃²⁺-AuNPs-peptide as ECL probe is evident.

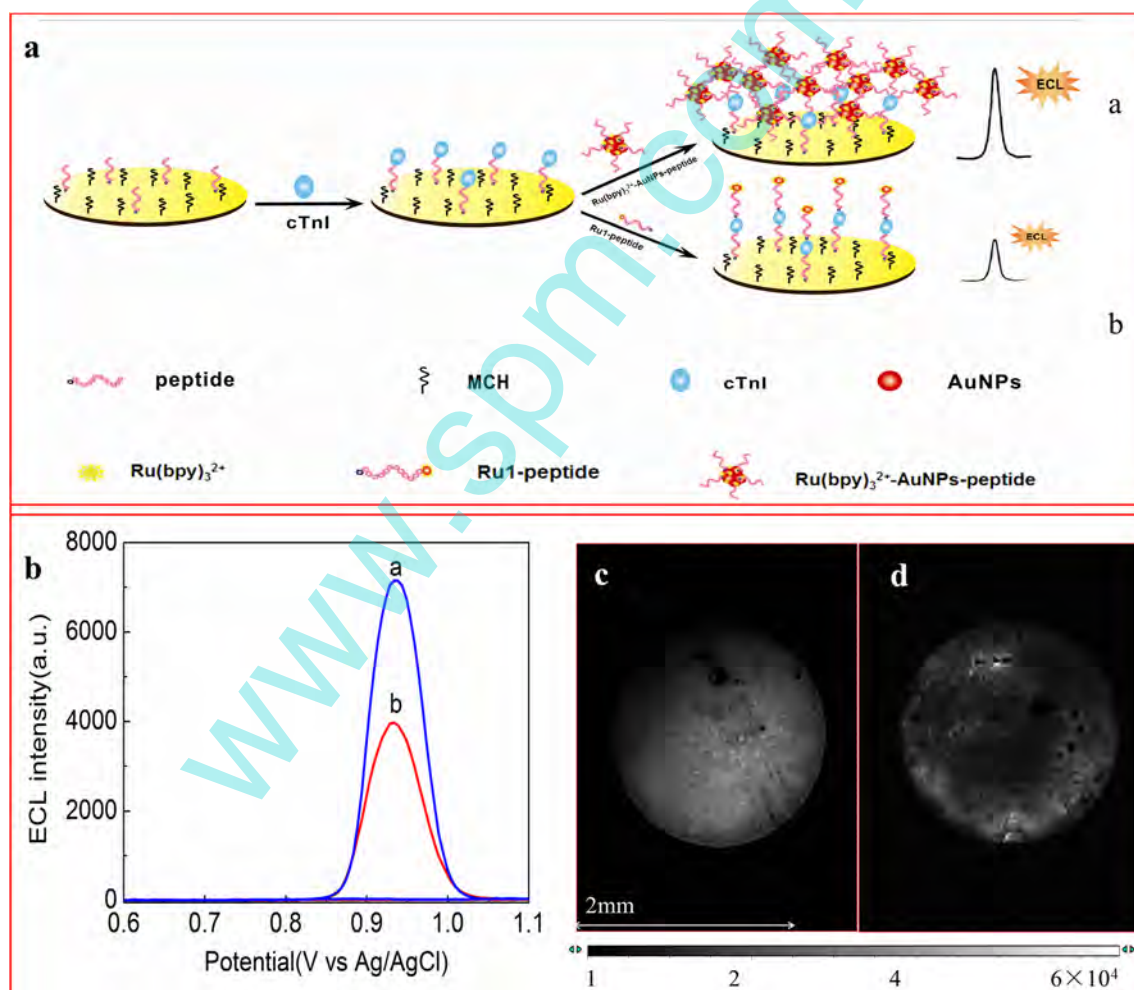


Fig. 4 **a** Schemes of two ECL bioassay for cTnI. **b** ECL intensity-potential profiles of peptide-modified electrode using Ru(bpy)₃²⁺-AuNPs-peptide (**a**) and Ru1-peptide (**b**) as ECL probes. **a** 7.0×10^{-11} g mL⁻¹ cTnI and **b** 7.0×10^{-10} g mL⁻¹ cTnI. **c** ECL image of the peptide-modified electrode after incubation with 7.0×10^{-11} g mL⁻¹ cTnI

using Ru(bpy)₃²⁺-AuNPs-peptide as ECL probe. **d** ECL image of the peptide-modified electrode after incubation with 7.0×10^{-10} g mL⁻¹ cTnI using Ru1-peptide as ECL probe. The measurement conditions: 0.10 M PBS (pH 7.4) containing 50 mM TPA. Scan rate at 100 mV s⁻¹

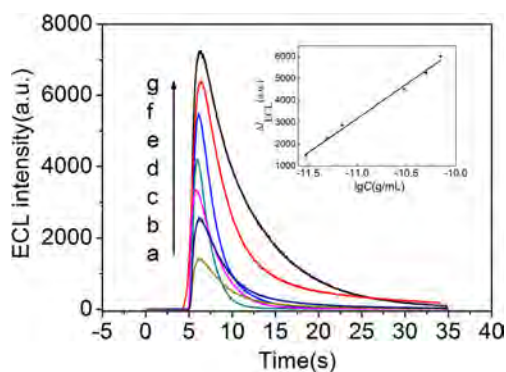


Fig. 5 ECL profiles of the peptide-modified electrode after incubation with different concentrations of cTnI. The calibration curve of cTnI (*inset*). The concentrations of cTnI: **a** blank, **b** 3.0×10^{-12} g mL $^{-1}$, **c** 5.0×10^{-12} g mL $^{-1}$, **d** 7.0×10^{-12} g mL $^{-1}$, **e** 3.0×10^{-11} g mL $^{-1}$, **f** 5.0×10^{-11} g mL $^{-1}$, and **g** 7.0×10^{-11} g mL $^{-1}$. The measurement conditions: 0.10 M PBS (pH 7.4) containing 50 mM TPA, applied potential, 0.95 V

Analytical performance for the determination of cTnI

Experimental parameters including applied potential and incubation time were optimized; 0.95 V was chosen as the applied potential and 60 min was employed as the incubation time in order to obtain a high sensitivity (see Fig. S5 in Supporting Information). Figure 5 shows the ECL profiles of the peptide-modified electrode after incubation with different concentrations of cTnI under the optimized conditions. The ECL intensity increased with increased cTnI concentrations and was directly related to the logarithm of the concentration of cTnI in the range of $3.0 \times 10^{-12} \sim 7.0 \times 10^{-11}$ g mL $^{-1}$. The linear regression equation was $\Delta I = 37708 + 3138 \lg C$ (unit of C is g mL $^{-1}$) with a correlation coefficient of 0.9954. The detection limit was 0.5 pg mL^{-1} ($S/N=3$). The proposed method exhibited more excellent analytical properties compared with other reported method for the detection of cTnI (Table 1). For example, the detection limit was 240-fold lower

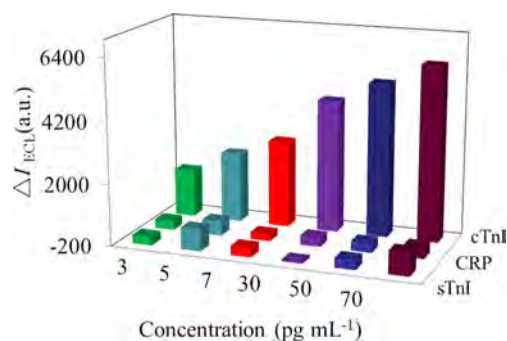


Fig. 6 The increased ECL intensities at the peptide-modified electrode after incubation with different concentrations of cTnI/CRP/sTnI. Measurement conditions are the same as those in Fig. 5

than that obtained by homogenous ECL method in our previous report using Ru1-labeled peptide [20] and nearly 10-fold lower than that obtained by ECL method in our previous report using liposome as carrier [21]. The relative standard deviation (RSD) for 5.0×10^{-12} g mL $^{-1}$ cTnI was 4.3 % ($n=5$). The ECL response for 5.0×10^{-12} g mL $^{-1}$ cTnI did not significantly change when stored in 10 mM PB (pH 7.4) at 4 °C for 10 days (RSD=6.4 %).

To assess the selectivity of the ECL-PB biosensing method, we attempted to determine cTnI in the presence of CRP, a specific marker for coronary events, sTnI, an isoform of troponin I, and other proteins including IgG, BSA, albumin chicken egg protein, and PSA. As shown in Fig. 6, a significant increase in the ECL signal was induced by the interaction of the peptide-modified electrode with cTnI compared to that for CRP and sTnI. Moreover, the ECL intensities increased with increased concentrations of cTnI. No obvious increases for CRP and sTnI were observed with increased concentrations of CRP and sTnI from 3.0×10^{-12} to 7.0×10^{-11} g mL $^{-1}$. Therefore, the developed strategy has sufficient selectivity, and cTnI could be unequivocally identified in the presence

Table 1 Analytical performance for cTnI

Detection technique	Recognition molecular	Amplify	Linear range	DL	References
Colorimetric	Antibody	Gold nanoparticle	–	0.3 ng mL $^{-1}$	[4]
Colorimetric	Antibody	Gold nanoparticle	0.01–5 ng mL $^{-1}$	0.01 ng mL $^{-1}$	[5]
Fluorescence	Antibody	Dyed nanoparticle	0.003–9.6 $\mu\text{g L}^{-1}$	0.0020 $\mu\text{g L}^{-1}$	[7]
EC	Peptide	–	0–10 $\mu\text{g mL}^{-1}$	0.34 $\mu\text{g mL}^{-1}$	[1]
EC	Antibody	Gold nanoparticles	0.2–12.5 ng mL $^{-1}$	0.2 ng mL $^{-1}$	[8]
EC	Antibody	Enzyme	0.2–10 ng mL $^{-1}$	148 pg mL $^{-1}$	[9]
CL	Antibody	Gold nanoparticles	0.1–100 ng mL $^{-1}$	0.027 ng mL $^{-1}$	[10]
ECL	Antibody	Gold nanoparticles	0.1–1000 ng mL $^{-1}$	0.06 ng mL $^{-1}$	[11]
ECL	Antibody	Gold nanoparticles	2.5–10,000 pg mL $^{-1}$	2 pg mL $^{-1}$	[12]
ECL	Peptide	–	0.78–78 ng mL $^{-1}$	0.12 ng mL $^{-1}$	[20]
ECL	Peptide	Liposome	0.01–5.0 ng mL $^{-1}$	4.5 pg mL $^{-1}$	[21]
ECL	Peptide	Gold nanoparticles	3.0–70 pg mL $^{-1}$	0.5 pg mL $^{-1}$	This work

EC electrochemistry, CL chemiluminescence

of CRP and sTnI. A significant increase for 5.0×10^{-11} g mL⁻¹ cTnI was obtained ($\Delta I = 5268$), while a slight increase in the ECL intensity for 1.0×10^{-9} g mL⁻¹ of other proteins was found (BSA ($\Delta I = 195$), PSA ($\Delta I = 195$), IgG ($\Delta I = 391$), and egg protein ($\Delta I = 433$), see Fig. S6 in Supporting Information). Clearly, these proteins did not interfere with the detection of cTnI. These results prove that the specific peptide selected by phage display technology has sufficient affinity for cTnI.

Conclusion

Here, a sensitive and simple ECL peptide-based biosensing method for cTnI was developed by incorporating Ru(bpy)₃²⁺-AuNPs-peptide as an ECL nanoprobe and a specific peptide as a molecular recognition element. Notably, AuNPs not only can capture numerous signal-generating molecules, resulting in high ECL intensity, but also can capture a significant amount of the peptide, providing poly binding motif. This novel Ru(bpy)₃²⁺-AuNPs-peptide probe displayed better ECL responses than the RuI-labeled peptide probe. A low detection limit of 0.5 pg mL⁻¹ was obtained for cTnI. Additionally, the proposed method is simple and time-saving because it avoids the complicated, uncontrollable synthesis of functional nanoparticles. Moreover, it utilizes a facile labeling procedure compared with other multi-label strategies involved in most ruthenium complex-encapsulated liposomes. Finally, the utilization of sandwich model could enhance the selectivity of the biosensor of cTnI. The strategy presented here could be easily extended to develop other ECL and electrochemical biosensing methods for other disease-related proteins.

Acknowledgments Financial support from The National Science Foundation of China (nos. 21475082, 21375084, 21275095), the Natural Science Basic Research Plan in Shaanxi Province of China (nos. 2013KJXX-73, 2014LQ2065, 2013SZS08-Z01), and Program for Innovative Research Team in Shaanxi Province (No. 2014KCT-28) are greatly acknowledged.

Open Access This article is distributed under the terms of the Creative Commons Attribution License which permits any use, distribution, and reproduction in any medium, provided the original author(s) and the source are credited.

References

1. Wu J, Crokek DM, West AC, Banta S (2010) Development of a troponin I biosensor using a peptide obtained through phage display. *Anal Chem* 82:8235–8243
2. Akanda MR, Aziz MA, Jo K, Tamilavan V, Hyun MH, Kim S, Yang H (2011) Optimization of phosphatase- and redox cycling-based immunosensors and its application to ultrasensitive detection of troponin I. *Anal Chem* 83:3926–3933
3. McDonnell B, Hearty S, Leonard P, O’Kennedy R (2009) Cardiac biomarkers and the case for point-of-care testing. *Clin Biochem* 42: 549–561
4. Guo H, Yang D, Gu C, Bian Z, He N, Zhang J (2005) Development of a low density colorimetric protein array for cardiac troponin I detection. *J Nanosci Nanotechnol* 5:2161–2166
5. Wu WY, Bian ZP, Wang W, Wang W, Zhu JJ (2010) PDMS gold nanoparticle composite film-based silver enhanced colorimetric detection of cardiac troponin I. *Sensors Actuators B* 147:298–303
6. Nandhikonda P, Heagy MD (2011) An abiotic fluorescent probe for cardiac troponin I. *J Am Chem Soc* 133:14972–14974
7. Järvenpää ML, Kuningas K, Niemi I, Hedberg P, Ristiniemi N, Pettersson K, Lövgren T (2012) Rapid and sensitive cardiac troponin I immunoassay based on fluorescent europium(III)-chelated nanoparticles. *Clin Chim Acta* 414:70–75
8. Bhalla V, Carrara S, Sharma P, Nangia Y, Suri CR (2012) Gold nanoparticles mediated label-free capacitance detection of cardiac troponin I. *Sensors Actuators B* 161:761–768
9. Ko S, Kim B, Jo SS, Oh SY, Park JK (2007) Electrochemical detection of cardiac troponin I using a microchip with the surface-functionalized poly(dimethylsiloxane) channel. *Biosens Bioelectron* 23:51–59
10. Cho IH, Paek EH, Kim YK, Kim JH, Paek SH (2009) Chemiluminometric enzyme-linked immunosorbent assays (ELISA)-on-a-chip biosensor based on cross-flow chromatography. *Anal Chim Acta* 632:247–255
11. Li F, Yu Y, Cui H, Yang D, Bian Z (2013) Label-free electrochemiluminescence immunosensor for cardiac troponin I using luminol functionalized gold nanoparticles as a sensing platform. *Analyst* 138:1844–1850
12. Shen W, Tian D, Cui H, Yang D, Bian Z (2011) Nanoparticle-based electrochemiluminescence immunosensor with enhanced sensitivity for cardiac troponin I using N-(aminobutyl)-N-(ethylisoluminol)-functionalized gold nanoparticles as labels. *Biosens Bioelectron* 27:18–24
13. Sun D, Hamlin D, Butterfield A, Watson DE, Smith HW (2010) Electrochemiluminescent immunoassay for rat skeletal troponin I (Tnni2) in serum. *J Pharmacol Toxicol Methods* 61:52–58
14. Zhou Y, Zhuo Y, Liao N, Chai Y, Yuan R (2014) Ultrasensitive electrochemiluminescent detection of cardiac troponin I based on a self-enhanced Ru(II) complex. *Talanta* 129:219–226
15. Hu L XG (2010) Applications and trends in electrochemiluminescence. *Chem Soc Rev* 39:3275–3304
16. Miao W (2008) Electrogenenerated chemiluminescence and its biorelated applications. *Chem Rev* 108:2506–2553
17. Iqbal SS, Mayo MW, Bruno JG, Bronk BV, Batt CA, Chambers JP (2000) A review of molecular recognition technologies for detection of biological threat agents. *Biosens Bioelectron* 15:549–578
18. Petrenko VA, Vodyanoy VJ (2003) Phage display for detection of biological threat agents. *J Microbiol Meth* 53:253–262
19. Park JP, Crokek DM, Banta S (2010) High affinity peptides for the recognition of the heart disease biomarker troponin I identified using phage display. *Biotechnol Bioeng* 105:678–686
20. Wang C, Qi H, Qiu X, Gao Q, Zhang C (2012) Homogeneous peptide-based electrogenerated chemiluminescence method for determination of troponin I. *Anal Methods* 4:2469–2474
21. Qi H, Qiu X, Xie D, Ling C, Gao Q, Zhang C (2013) Ultrasensitive electrogenerated chemiluminescence peptide-based method for the determination of cardiac troponin I incorporating amplification of signal reagent-encapsulated liposomes. *Anal Chem* 85:3886–3894
22. Mirkin CA, Letsinger RL, Mucic RC, Strohoff JJ (1996) A DNA-based method for rationally assembling nanoparticles into macroscopic materials. *Nature* 382:607–609

23. Qi H, Peng Y, Gao Q, Zhang C (2009) Applications of nanomaterials in electrogenerated chemiluminescence biosensors. *Sensors* 9:674–695
24. Cao X, Ye Y, Liu S (2011) Gold nanoparticle-based signal amplification for biosensing. *Anal Biochem* 417:1–16
25. Guo Y, Guo S, Fang Y, Dong S (2010) Gold nanoparticle/carbon nanotube hybrids as an enhanced material for sensitive amperometric determination of tryptophan. *Electrochim Acta* 55:3927–3931
26. Thavanathan J, Huang NM, Thong KL (2014) Colorimetric detection of DNA hybridization based on a dual platform of gold nanoparticles and grapheneoxide. *Biosens Bioelectron* 55:91–98
27. Shan M, Li M, Qiu X, Qi H, Gao Q, Zhang C (2014) Sensitive electrogenerated chemiluminescence peptide-based biosensor for the determination of troponin I with gold nanoparticles amplification. *Gold Bull* 47:57–64
28. Tian DY, Duan CF, Wang W, Cui H (2010) Ultrasensitive electrochemiluminescence immunosensor based on luminol functionalized gold nanoparticle labeling. *Biosens Bioelectron* 25:2290–2295
29. Duan R, Zhou X, Xing D (2010) Electrochemiluminescence barcode method based on cysteamine-gold nanoparticle conjugates. *Anal Chem* 82:3099–3103
30. Tokel NE, Bard AJ (1972) Electrogenerated chemiluminescence. IX. Electrochemistry and emission from systems containing Tris(2,2'-bipyridine)ruthenium(II) dichloride. *J Am Chem Soc* 94:2862–2863
31. Sun X, Du Y, Dong S, Wang E (2005) Method for effective immobilization of Ru(bpy)₃²⁺ on an electrode surface for solid-state electrochemiluminescence detection. *Anal Chem* 77:8166–8169
32. Zhang L, Xu Z, Sun X, Dong S (2007) A novel alcohol dehydrogenase biosensor based on solid-state electrogenerated chemiluminescence by assembling dehydrogenase to Ru(bpy)₃²⁺-Au nanoparticles aggregates. *Biosens Bioelectron* 22:1097–1100
33. Mao L, Yuan R, Chai Y, Zhuo Y, Yang X, Yuan S (2010) Multi-walled carbon nanotubes and Ru(bpy)₃²⁺/nano-Au nano-sphere as efficient matrixes for a novel solid-state electrochemiluminescence sensor. *Talanta* 80:1692–1697
34. Li M, Zhang M, Ge S, Yan M, Yu J, Huang J, Liu S (2013) Ultrasensitive electrochemiluminescence immunosensor based on nanoporous gold electrode and Ru-AuNPs/graphene as signal labels. *Sensors Actuators B Chem* 181:50–56
35. Wu M, He L, Xu JJ, Chen H (2014) RuSi@Ru(bpy)₃²⁺/Au@Ag₂S nanoparticles electrochemiluminescence resonance energy transfer system for sensitive DNA detection. *Anal Chem* 86:4559–4565
36. Li M, Nie M, Wu Z, Liu X, Chen G (2011) Colorimetric and luminescent bifunctional Ru(II) complex-modified gold nanoprobe for sensing of DNA. *Biosens Bioelectron* 29:109–114
37. Gui G, Zhuo Y, Chai Y, Liao N, Zhao M, Han J, Zhu Q, Yuan R, Xiang Y (2013) Supersandwich-type electrochemiluminescent aptasensor based on Ru(phen)₃²⁺ functionalized hollow gold nanoparticles as signal-amplifying tags. *Biosens Bioelectron* 47:524–529
38. Elmes RBP, Orange KN, Cloonan SM, Williams DC, Gunnlaugsson T (2011) Luminescent ruthenium(II) polypyridyl functionalized gold nanoparticles; their DNA binding abilities and application as cellular imaging agents. *J Am Chem Soc* 133:15862–15865
39. Frens G (1973) Controlled nucleation for the regulation of the particle size in monodisperse gold suspensions. *Nat Phys Sci* 241:20–22
40. Carvalho RF, Freire RS, Kubota LT (2005) Polycrystalline gold electrodes: a comparative study of pretreatment procedures used for cleaning and thiolself-assembly monolayer formation. *Electroanalysis* 17:1251–1259
41. Patil S, Datar S, Rekha N, Asha SK, Dharmadhikari CV (2013) Charge storage and electron transport properties of gold nanoparticles decorating a urethane-methacrylate comb polymer network. *Nanoscale* 5:4404–4411
42. Grabar KC, Freeman RG, Hommer MB, Natan MJ (1995) Preparation and characterization of Au colloid monolayers. *Anal Chem* 67:735–743
43. Brust M, Bethell D, Schiffrin DJ, Kiely C (1995) Novel gold-dithiolnano-networks with non-metallic electronic properties. *Adv Mater* 7:795–797
44. Qi H, Ling C, Huang R, Qiu X, Shangguan L, Gao Q, Zhang C (2012) Functionalization of single-walled carbon nanotubes with protein by click chemistry as sensing platform for sensitized electrochemical immunoassay. *Electrochim Acta* 63:76–82
45. Bardea A, Katz E, Willner I (2000) Probing antigen-antibody interactions on electrode supports by the biocatalyzed precipitation of an insoluble product. *Electroanalysis* 14:1097–1106
46. Jena BK, Raj CR (2006) Electrochemical biosensor based on integrated assembly of dehydrogenase enzymes and gold nanoparticles. *Anal Chem* 78:6332–6339
47. Miao W, Choi JP, Bard AJ (2002) Electrogenerated chemiluminescence 69: the tris(2,2'-bipyridine)ruthenium(II), (Ru(bpy)₃²⁺)/Tri-n-propylamine (TPrA) system revisited—a new route involving TPrA^{•+} cation radicals. *J Am Chem Soc* 124:14478–14485
48. Engstrom RC, Johnson KW, DesJarlais S (1987) Characterization of electrode heterogeneity with electrogenerated chemiluminescence. *Anal Chem* 59:670–673
49. Terskikh AV, Le Doussal JM, Cramer R, Fisch I, Mach JP, Kajava AV (1997) “Peptabody”: a new type of high avidity binding protein. *Proc Natl Acad Sci* 94:1663–1668
50. Vance D, Shah M, Joshi A, Kane RS (2008) Polyvalency: a promising strategy for drug design. *Biotechnol Bioeng* 101:429–434
51. Chen ZY (2007) Gold nanoparticle-modified ITO electrode for electrogenerated chemiluminescence: well-preserved transparency and highly enhanced activity. *Langmuir* 23:11387–11390